ChemPhotoChem

Chemistry Europe
European Chemical Societies Publishing
ChemPhotoChem

RESEARCH ARTICLE OPEN ACCESS

Novel Photoinitiators for Two-Step Absorption-Based 3D Laser Nanoprinting: From Molecular Design to Printing Behavior

Aleksandra Vranic[1] | Sarah Wulff[1] | Pascal Rietz[2,3] | Jonathan L. G. Schneider[3] | Sophia Abou El Mirate[1] | Martin Wegener[2,3] | Stefan Bräse[1,4]

[1]Institute of Organic Chemistry (IOC), Karlsruhe Institute of Technology (KIT), Karlsruhe, Germany | [2]Institute of Nanotechnology (INT), Karlsruhe Institute of Technology (KIT), Karlsruhe, Germany | [3]Institute of Applied Physics (APH), Karlsruhe Institute of Technology (KIT), Karlsruhe, Germany | [4]Institute of Biological and Chemical Systems – Functional Molecular Systems (IBCS-FMS), Karlsruhe Institute of Technology (KIT), Karlsruhe, Germany

Correspondence: Stefan Bräse (stefan.braese@kit.edu)

Received: 3 October 2025 | **Revised:** 7 December 2025 | **Accepted:** 11 December 2025

Keywords: 3D laser nanoprinting | photoinitiator | photoresists | two-step absorption

ABSTRACT

Using two-step absorption instead of two-photon absorption in 3D laser nanoprinting reduces demands on necessary laser systems but still poses a challenge for chemistry. Photoresists consisting of a photoinitiator and a viscous monomer are hardened through photopolymerization with one or two different laser sources. Until now, the influence of the photoinitiator type on printing behavior has remained unclear, limiting the rational design of new materials. In this study, we demonstrate a direct connection between molecular design and printing performance, providing new insights that guide the targeted development of novel photoinitiators. One essential parameter in designing new photoinitiators is the laser power required to initiate photopolymerization, which varies with molecular size, regioisomeric substitution, and substituent type. Screenings in this and a previous study about two-step absorption show that, thus far, the only applicable molecules for this specific 3D printing technique are 1,2-diketones, primarily benzil derivatives. These compounds are mainly synthesized using a Sonogashira cross-coupling reaction followed by an oxidation of the resulting triple bond. The photoinitiators introduced in this work can be referred to as two-step, one-color systems, allowing 3D structures to be printed using only a single 405 nm laser source.

1 | Introduction

Light-induced 3D printing is emerging as a rapidly advancing and increasingly significant field of research [1, 2]. Techniques used can be divided into three main parts: stereolithography (SLA), digital light processing (DLP), and direct laser writing (DLW) [3, 4]. SLA is one of the earliest experimentally realized light-induced 3D printing techniques, consisting of a light source, a container with liquid photoresist, and a build platform. When irradiated with light, the photoresist changes from a liquid to a solid at the exposed points or regions in space. This enables the 3D-printed structure to be built up in a layer-by-layer approach [5]. Similar to SLA, DLP uses a larger light projection to solidify an entire layer of liquid photoresist at once, rather than point by point. This allows higher printing speeds with consistent accuracy [3].

The most prominent representative of DLW is based on two-photon absorption [6] of light. In this technique, focused femtosecond pulsed laser beams create structures within a viscous medium that is located on a glass substrate. Photopolymerization occurs because the electron population of the molecules is excited from the ground state to a higher energy level, from which radicals are generated to initiate the polymerization chain. To reach this excited state, two photons must be absorbed. The absorption of the first photon excites an electron from the ground state to a virtual

intermediate state. Only if a second photon is absorbed while the electron is in this virtual state, radicals are generated, initiating photopolymerization. This polymerization occurs only at the laser's focal point, where the probability of two-photon absorption is highest, confining the reaction to a very small volume called a "voxel." This confinement enables the fabrication of 3D structures with dimensions ranging from the nano- to micrometer scale [7–10].

Besides this well-known way of 3D laser nanoprinting, two-photon absorption forms the basis for related approaches in which initiator molecules are excited through a similar pathway. One such approach employed in this work is two-step absorption (Figure 1) [11].

In this process, the previously mentioned virtual intermediate state in two-photon absorption is replaced by a real intermediate state (S_1 and T_1). This means that two photons can be absorbed sequentially at different points in time instead of simultaneously. A virtue of this approach is that less expensive and more compact low-power continuous-wave (cw) lasers can be used. Since there are two separate absorption steps, two cw lasers with different wavelengths can also be used to excite the initiator. The printing materials are photoresists consisting of a photoinitiator (PI, e.g., 1,2-diketones) that gets excited by the photon energy and starts the polymerization, and a liquid monomer (e.g., pentaerythritol triacrylate, PETA). Scavengers such as 2,2,6,6-tetramethylpiperidinyloxyl (TEMPO) have to be added to prevent side reactions.

In addition to the two pioneering molecules biacetyl [12] and benzil [11], several other 1,2-diketone-based photoinitiators are known that are suitable for this type of 3D laser nanoprinting [13]. However, a clear understanding of how molecular structure influences individual printing parameters, such as the laser power required for photopolymerization, has been lacking so far [14]. This work introduces a wide range of new photoinitiator molecules differing in size, substituents, and substitution positions, and experimentally analyzes how these variations affect printing performance.

2 | Molecular Design

As previous studies [11–13] have shown, 1,2-diketones have so far been the only applicable class of photoinitiator for 3D laser nanoprinting via two-step absorption. Although a variety of commercially available molecules, such as disulfides, imines, and biphenyls, were tested within this work, none proved suitable for 3D laser nanoprinting due to poor solubility or undesired background polymerization. Cyclic and aliphatic diketones were either synthetically unavailable or proved unsuitable for this application. As a result, the focus was placed on 1,2-diketones, particularly benzil derivatives. Figure 2 provides an overview of previously reported photoinitiators that are suitable for this application, alongside examples of commercially available compounds that were found to be unsuitable.

The benzil derivatives were synthesized with one out of four possible routes: Sonogashira cross-coupling [15, 16] or Stille cross-coupling [17] followed by an oxidation [18] of the triple bond, Suzuki cross-coupling [19], or benzoin condensation followed by an oxidation of the hydroxy group. All four pathways are visualized in Scheme 1.

The primary reaction employed in this work is the Sonogashira cross-coupling, in which an aryl halide reacts with an aryl alkyne to form a coupled alkyne intermediate [15, 16, 20]. This intermediate is subsequently oxidized using palladium(II) chloride and dimethyl sulfoxide (DMSO) to afford the target benzil derivative with high selectivity [18]. Extended bis-benzil derivatives were obtained using diethynylbenzenes as starting materials, while standard benzils were synthesized from unsubstituted and substituted ethynylbenzenes.

As an alternative route for alkyne synthesis, the Sonogashira reaction can be replaced by Stille cross-coupling. In this approach, symmetric organostannanes, such as bis(tributylstannyl)acetylene, are used to obtain symmetric alkyne derivatives. However, the high toxicity of the required organostannanes and associated environmental concerns limit the practical applicability of this method [17].

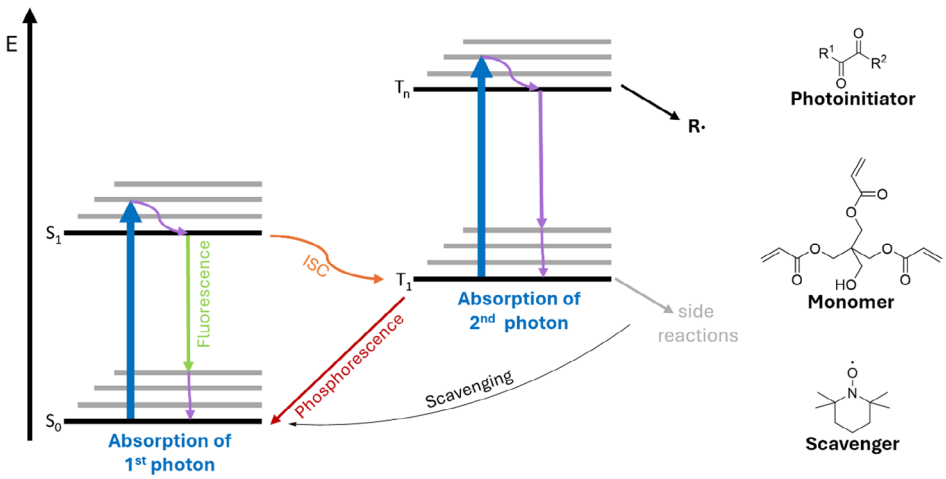

FIGURE 1 | Schematic representation of a two-step absorption process in a molecule. The first photon is absorbed from the ground state S_0 to the higher excited state S_1. After Intersystem Crossing (ISC) to T_1, a second photon can be absorbed with either the same or a different wavelength to a higher excited state T_n. From this state, radicals can be formed initiating photopolymerization. To prevent undesirable side reactions from T_1, a radical scavenger is added to the photoresist as a third component besides photoinitiator and monomer [11].

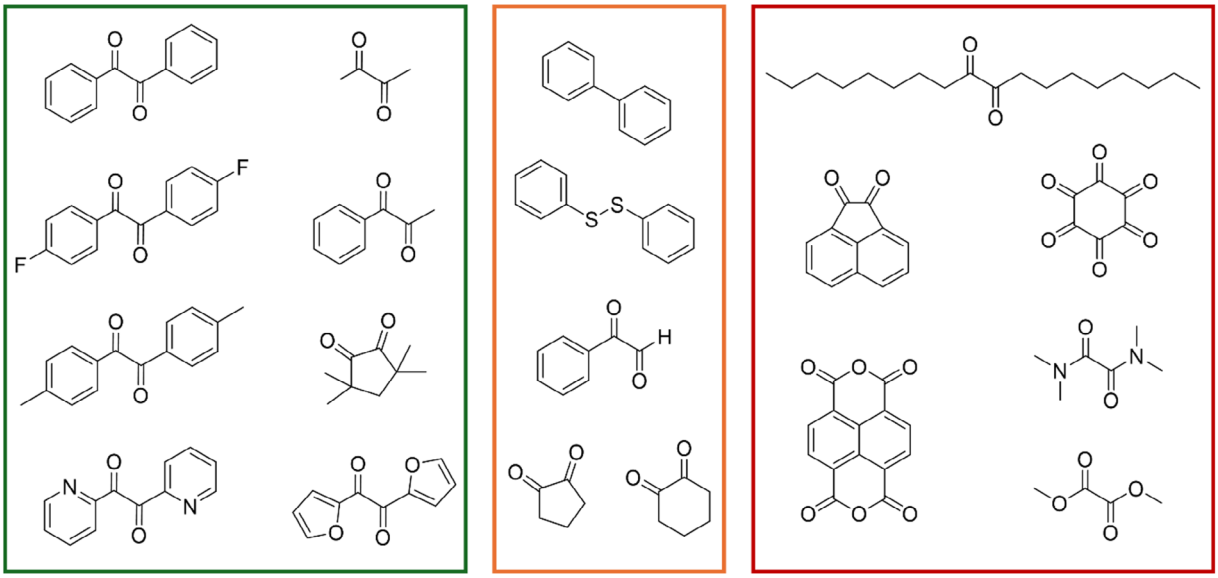

FIGURE 2 | Overview of selected previously reported photoinitiators suitable for this application (green), alongside compounds found to be unsuitable due to undesired polymerization (orange), or poor solubility in the monomer (red).

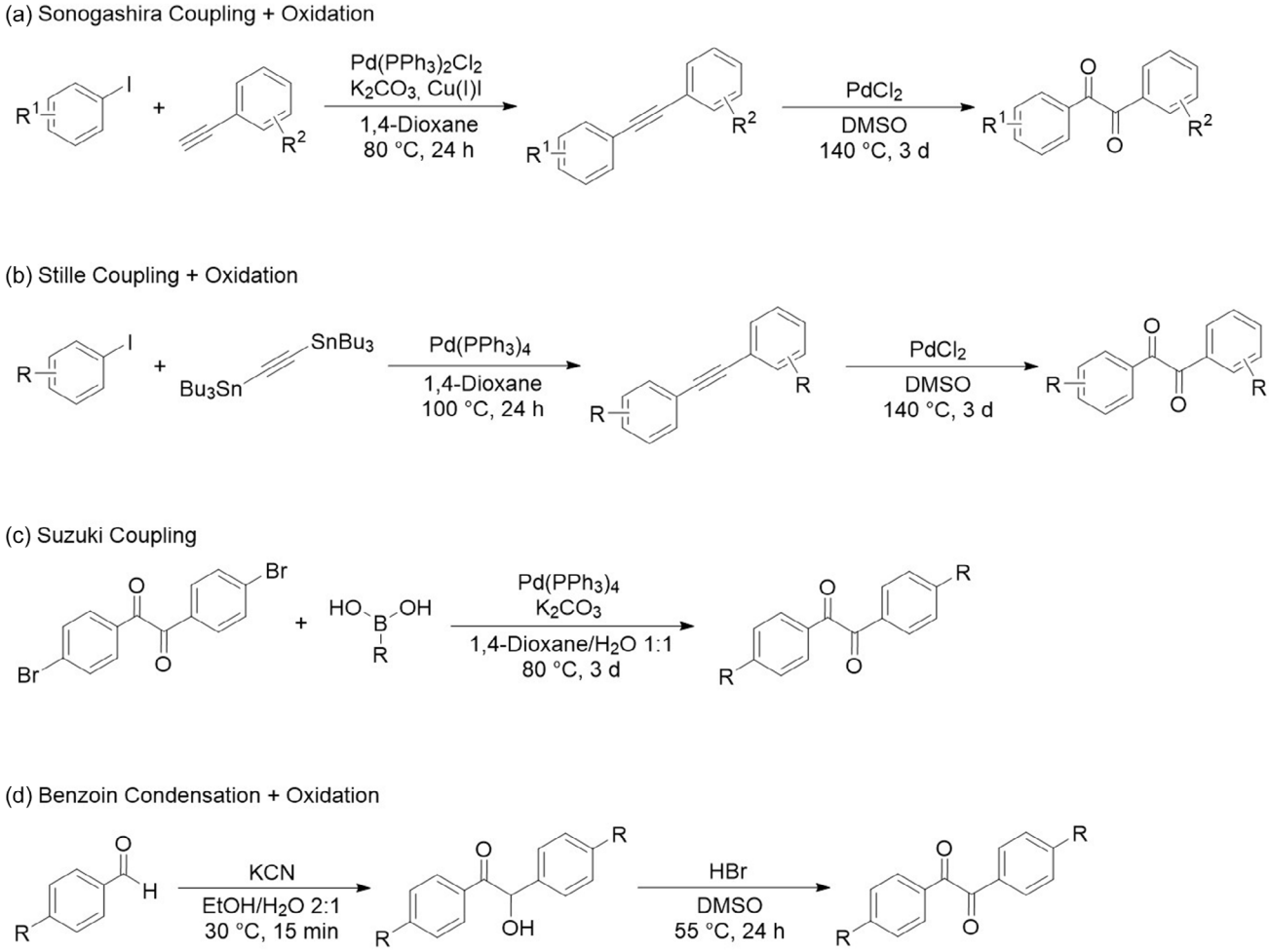

SCHEME 1 | Different approaches for the synthesis of several benzil-derivatives: (a) Sonogashira coupling followed by alkyne oxidation, (b) Stille coupling followed by alkyne oxidation, (c) Suzuki Coupling, and (d) Benzoin condensation followed by benzoin oxidation [15–19].

Another cross-coupling strategy applied in this study is the Suzuki reaction, where bromo-benzil derivatives are functionalized with boronic acid derivatives. This method allows the direct formation of the desired products in a single step, avoiding the need for intermediate oxidation, as illustrated in Scheme 1c [19, 20].

In addition to cross-coupling approaches, diketones can also be synthesized via benzoin condensation [21]. Here, two aldehyde molecules undergo a catalyzed condensation to form a benzoin intermediate, which is then oxidized [22] to the corresponding diketone, providing a straightforward alternative to cross-coupling methods.

The different reaction pathways presented in Scheme 1 provide access to distinct substitution patterns in 1,2-diketones. Pathways **c** and d lead exclusively to symmetric compounds bearing substituents in *para*-position, whereas pathway **b** also enables the synthesis of *meta*-substituted derivatives. In contrast, pathway a is unique in that it allows the preparation of both symmetric and asymmetric molecules with varying substituents and substitution patterns. Using these strategies, twenty-three novel 1,2-diketones were synthesized in this study. A wide variety of substituents was introduced to tune the properties of the resulting photoinitiators, including halides, methoxy or methyl groups, as well as (un)substituted phenyl rings. This approach further allowed the extension of benzil derivatives to systems containing three instead of two aromatic rings, referred to as "bis-benzil derivatives."

The obtained compounds are divided into four subgroups: benzils with substituents in *para*-position (**B1-1** to **B1-9**), benzils with substituents in *meta*-position (**B2-1** to **B2-5**), *meta*-linked bis-benzils (**B3-1** to **B3-5**), and *para*-linked bis- and tris-benzils (**B4-1** to **B4-4**) (Figure 3).

Table 1 summarizes key information for the compounds shown in Figure 3. For each photoinitiator, the table lists the synthetic route used and the overall yield. Additionally, it provides parameters relevant to 3D printing, including the concentration used in the photoresist and whether each molecule is able to initiate photopolymerization and thus produce stable 3D structures, listed as "3D printability." The latter two parameters are discussed in detail in Section 3.

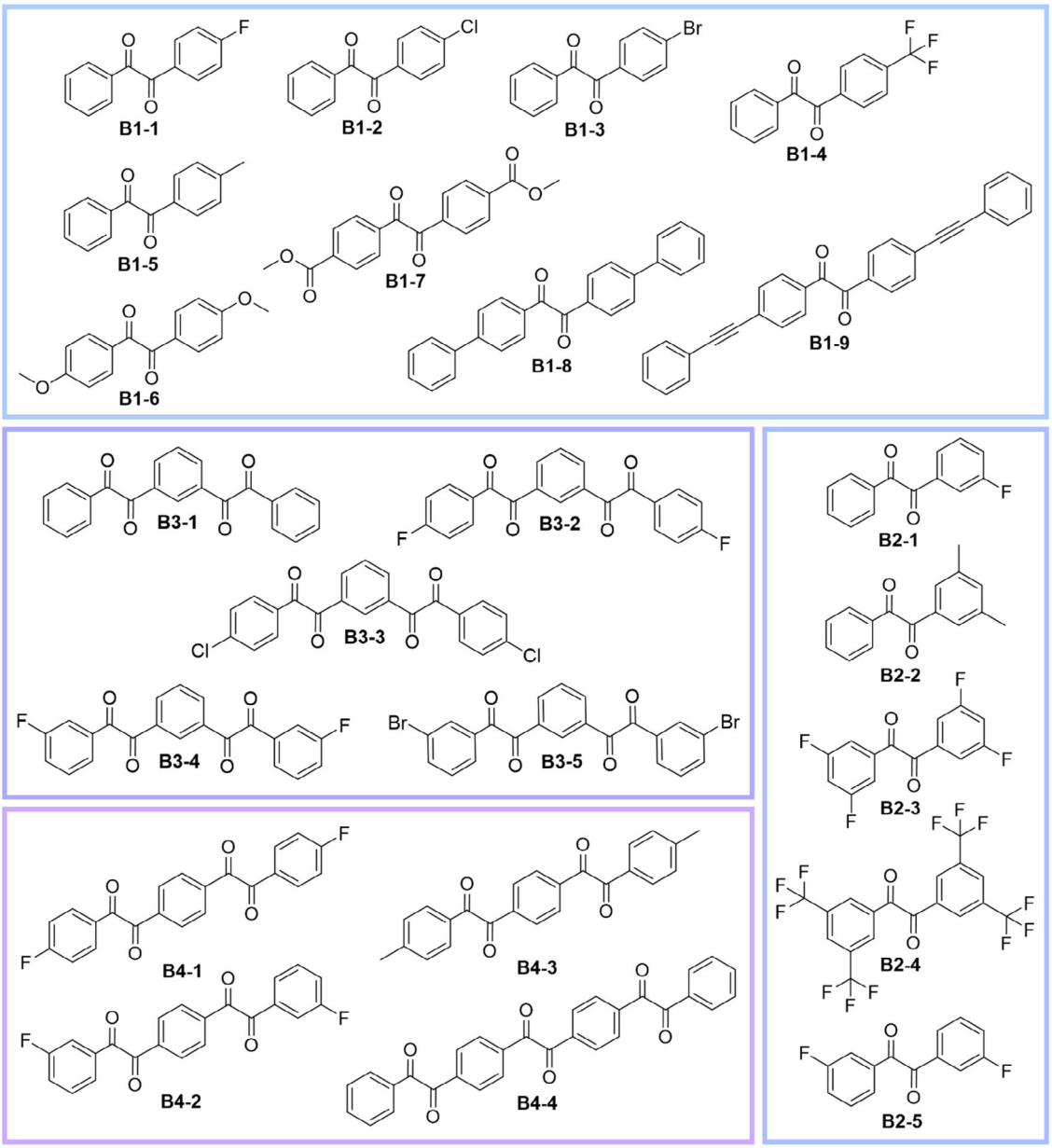

FIGURE 3 | Representation of the 23 novel synthesized benzil-derivatives within this work.

TABLE 1 | Key information for the synthesized compounds shown in Figure 3, including the method of synthesis, overall yield, solubility, concentration used in the photoresist, and suitability for 3D printing.

Abb.	Reaction	Yield, %	Concentration in photoresist, mM	3D Printablity
B1-1	Sonogashira + Oxidation	63	100	✓
B1-2	Sonogashira + Oxidation	79	100	✓
B1-3	Sonogashira + Oxidation	12	not soluble	—
B1-4	Sonogashira + Oxidation	24	100	✓
B1-5	Sonogashira + Oxidation	41	100	✓
B1-6	Stille + Oxidation	39	100	✓
B1-7	Benzoin Condensation + Oxidation	18	not soluble	—
B1-8	Suzuki	90	50	✓
B1-9	Sonogashira	33	not soluble	—
B2-1	Sonogashira + Oxidation	38	100	✓
B2-2	Sonogashira + Oxidation	42	100	—
B2-3	Sonogashira + Oxidation	66	100	✓
B2-4	Sonogashira + Oxidation	49	100	✓
B2-5	Stille + Oxidation	30	100	✓
B3-1	Sonogashira + Oxidation	36	100	✓
B3-2	Sonogashira + Oxidation	35	50	✓
B3-3	Sonogashira + Oxidation	39	not soluble	—
B3-4	Sonogashira + Oxidation	61	50	✓
B3-5	Sonogashira + Oxidation	33	not soluble	—
B4-1	Sonogashira + Oxidation	31	not soluble	—
B4-2	Sonogashira + Oxidation	5	not soluble	—
B4-3	Sonogashira + Oxidation	21	100	✓
B4-4	Oxidation	18	not soluble	—

Note: Starting material for **B4-4**.

Most of the synthesized compounds were obtained via Sonogashira cross-coupling followed by oxidation. A few exceptions include **B1-8**, which was prepared by a Suzuki cross-coupling, as well as **B1-6** and **B2-5**, which were synthesized via Stille coupling but suffered from lower yields due to impurities during the coupling step. **B1-7** represents the only compound synthesized without cross-coupling, using reaction type **d** (Figure 3), which also resulted in comparatively lower yields.

Detailed experimental procedures and analytical data for all compounds as well as data about an obtained crystal structure for **B2-1** are provided in the Supporting Information.

3 | Printing Behavior of Photoinitiators

This section will focus on key parameters that determine the suitability of different photoinitiators. One important aspect, shown in Table 1, is their printability. After the successful synthesis, the compounds were used for the preparation of new photoresists. The concentration of the photoinitiator affects various polymerization parameters, including conversion rate, cure depth, and crosslink density [23]. To ensure consistency and better comparability of the photoinitiators, this variable was kept constant. In accordance with previous publications on 1,2-diketones in two-step absorption-based 3D laser nanoprinting, a concentration of 100 mM was chosen. For PIs that were insoluble at this concentration, a dilution to 50 mM was performed, which is also consistent with previous publications [13]. The photoinitiators **B1-1, B1-2, B1-4, B1-6, B2-1, B2-2, B2-3, B2-4, B2-5, B3-1,** and **B4-3** were dissolved in the PETA at a concentration of 100 mM. **B1-8, B3-2,** and **B3-4** were diluted to a concentration of 50 mM to be soluble in PETA. **B1-3**, **B1-7**, **B1-9**, **B3-3**, **B3-5**, **B4-1,** and **B4-2** were not soluble even at a concentration of 12.5 mM. Although **B4-4** became soluble in PETA at 6 mM after further dilution, printing tests showed that at this concentration, no polymerization occurred, making higher dilution impractical. TEMPO was added to every photoresist as a scavenger in a ratio of 2:1 (PI:TEMPO). **B2-2** is the only soluble benzil that does not act as photoinitiator and therefore could not be used for photopolymerization. The reason **B2-2** does not act as a photoinitiator despite being soluble is unclear. One potential reason for this could be that the energy of the laser used might be insufficient to initiate bond cleavage and generate reactive radicals. Another possibility is that **B2-2** undergoes a different photochemical pathway than the two-step mechanism observed for other benzil derivatives. This could prevent polymerization initiation under the applied experimental conditions. An overview of the evaluated photoinitiators is provided in Table 1, where all entries

marked in the last column are 3D laser nanoprintable via two-step absorption.

Before printing 3D structures, each photoresist was investigated in a so-called dosetest with a velocity of 100 µm/s (Supporting Information, Figure 1). This dosetest is used to determine whether a photoresist can be polymerized with a single laser source or by simultaneously using two lasers of different wavelengths, specifically 405 and 637 nm, allowing the suitability of dual-wavelength excitation for printing to be assessed. To do so, dashed line patterns are printed at varying laser powers of the blue as well as the red laser source, following the protocol already described in [3, 4]. Here, the power of the first laser at 405 nm (blue) is kept constant, and the power of the second laser at 637 nm (red) varies. The resulting data are plotted with the blue laser power (P_{405}) on the vertical axis against the red laser power (P_{637}) on the horizontal axis. A decrease in the required blue laser power in the presence of the red laser indicates two-step two-color (2S2C) absorption behavior. In contrast, when no decrease is observed in P_{405} with increasing red laser power, the photoinitiator exhibits two-step one-color (2S1C) absorption behavior. It is crucial to acknowledge that the dosetests provide merely an initial indication of these effects. Evaluating the possibility of printing 3D structures provides more information about the process. However, in this study, the dose tests correspond to actual behavior. The photoinitiator with the most pronounced 2S2C-effect is the aliphatic diketone biacetyl (**BA).** The dosetest is illustrated under the same conditions as the diketones previously shown (**BA-1**) [13], as well as under the conditions that achieved the best results and were previously used for light-sheet 3D laser printing (**BA-2**) [12]. The latter is the only one printed under different conditions: a ratio of 10:1 of BA to TEMPO and a blue 440 nm laser. In Figure 4, the photoinitiators showing the strongest two-color behavior are plotted alongside BA for comparison. All dosetests can be found in Figure 2 of the Supporting Information.

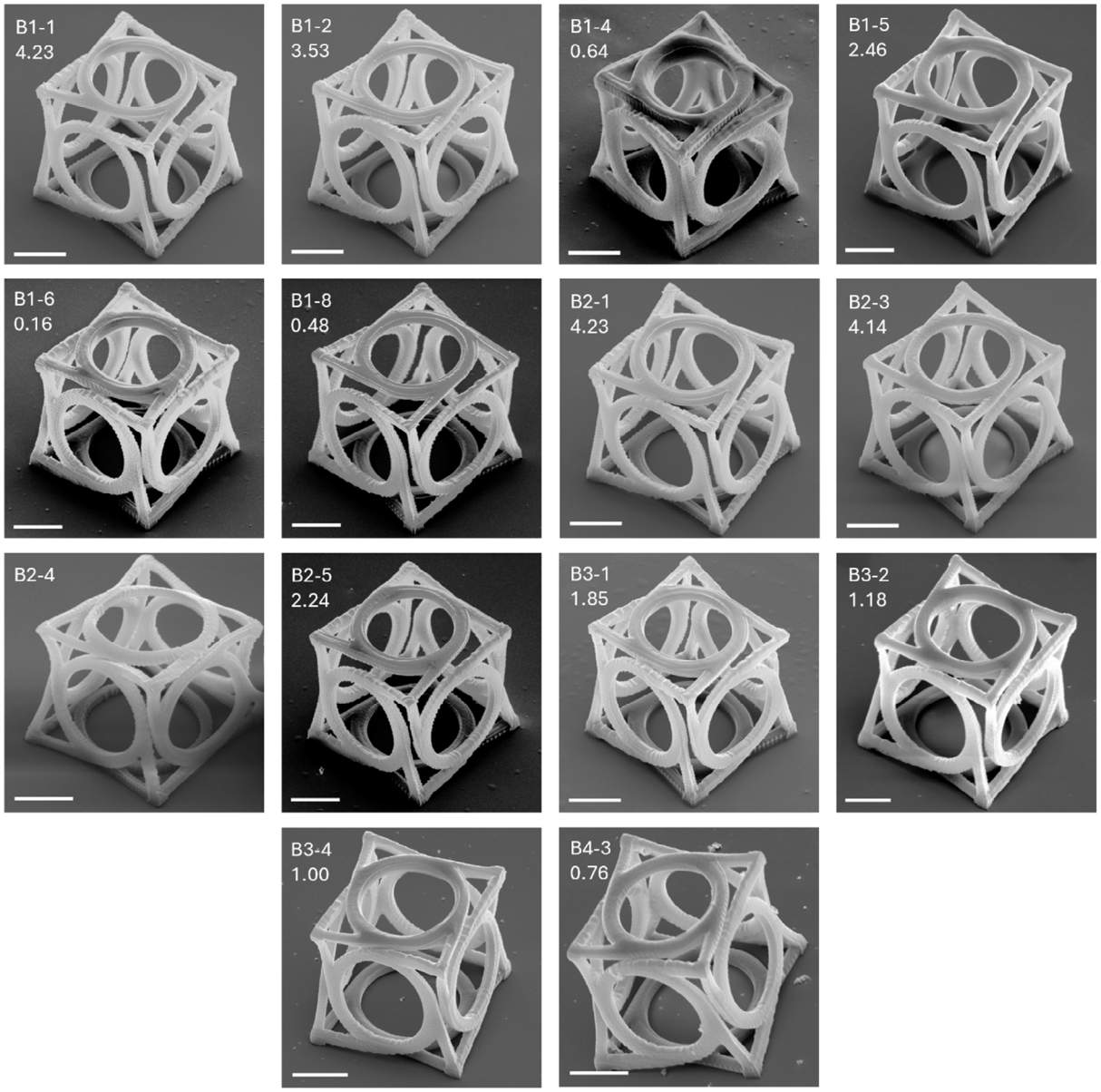

FIGURE 4 | Printed 3D structures of every photoresist shown in this work. Below the abbreviation for the photoresist, we denote the laser power used in units of mW. For all images, the scale bars correspond to 5 µm.

As depicted in Figure 5, none of the synthesized PIs exhibit a comparable decrease in the blue laser power like **BA-1** and **BA-2** (yellow and orange curve). Using **BA-2** as photoinitiator in its best-performed conditions, the required blue laser power decreases from 67.57 μW to 1.85 μW when increasing the red laser power from 0.04 mW to 20 mW, corresponding to approximately a factor of 37. At the same time, **BA-1** in the conditions chosen for all PIs in this work, the required blue laser power decreases from 210.48 μW to 18.36 μW appropriate to a factor of around 11.5. The most pronounced decrease shown in this work was observed for **B1-2** and **B2-1**. The difference of the required blue laser power in presence of the red laser corresponds for both PIs to a factor of around 7, while P_{405} decreases from 52.36 μW to 7.12 μW for **B1-2** and from 128.44 μW to 18.29 μW for **B2-1**. Although there are visible decreases and influence of the red laser for each PI, the strongest two-color effect is four times smaller than the best of **BA** and smaller for **BA** in the same conditions. Therefore, the PIs presented in this study cannot compete with **BA** and are not suitable for printing techniques such as light-sheet printing, where a photopolymerization with two wavelengths is necessary. However, the graphical analysis also reveals the laser power needed to initiate photopolymerization.

Comparing the benzil derivatives **B2-1**, **B2-3,** and **B2-5**, which are functionalized with different numbers of fluorine substituents in the *meta*-position, they show the trend that the required laser power increases with the number of fluorine atoms. The benzil derivative **B2-3** with the most fluorine substituents requires the highest laser power, with a minimum of 64.87 μW to initiate the photopolymerization, while PI **B2-1,** only functionalized with one fluorine, requires the least, with 18.29 μW. The strong negative inductive effect of aromatic fluorines can be an explanation for this finding. As the most electronegative atom, fluorine has the strongest -I-effect, removing σ-electron density and lowering the highest occupied molecular orbital (HOMO) of the molecular system. Withdrawing σ-electron density out of the aromatic ring lowers the HOMO-energy of the molecular system. For compounds with small π-systems, the effective excitation energy is increased with more fluorine atoms, making the PI less reactive. The same reasoning can explain the behavior of the two *para*-substituted benzils **B1-1** and **B1-2**. Chlorine has a lower inductive effect compared to fluorine, making **B1-2** photopolymerizable with less laser power compared to **B1-1**.

Another factor impacting the laser power is the molecular architecture of the photoinitiator. Comparing **B3-1** and **B3-4**, which contain two benzil units instead of one, it becomes evident that molecules with multiple diketone moieties require less laser power to initiate photopolymerization. The presence of two benzil groups increases the probability that absorbed photons populate reactive excited states. At the same time, the interaction between both diketone units can lower the excitation energy and prolong the lifetime of the excited state. These effects enhance the efficiency of radical generation and thereby reduce the initiation threshold. In addition, the incorporation of polar substituents on bis-benzil, such as fluorine, seems to reduce the required laser power. It is assumed that the electronic structure is modulated by stabilizing excited states and facilitating charge–transfer processes [13, 24–26].

With the knowledge about photopolymerization behavior, 3D structures were printed using the fourteen soluble PIs. For each PI, the same 3D structure (chiral metamaterial cell, dimension 16 μm × 16 μm) was printed using the same parameters. After printing, the substrate was immersed in acetone for 5 minutes and isopropanol for 1 minute, then dried under a stream of nitrogen to develop the print and remove any unreacted photoresist. The substrate was then sputter-coated with gold and examined using scanning electron microscopy (SEM). Figure 4 displays the SEM images of one 3D structure for each photoinitiator, as well as the laser power in mW applied for this printing.

The advantages of 3D laser nanoprinting with lower energy include more energy-efficient printing, reduced stress on the optical setup, and easier fabrication of delicate nanostructures. Therefore, photoinitiators that require less power to achieve the same structural quality are more effective. The laser power shown for each structure corresponds to the conditions giving the best appearance, rather than the minimum required for polymerization. A quantitative evaluation of the line width from the 3D printed structures was not performed in this study. Instead, the printed features were examined qualitatively based on their

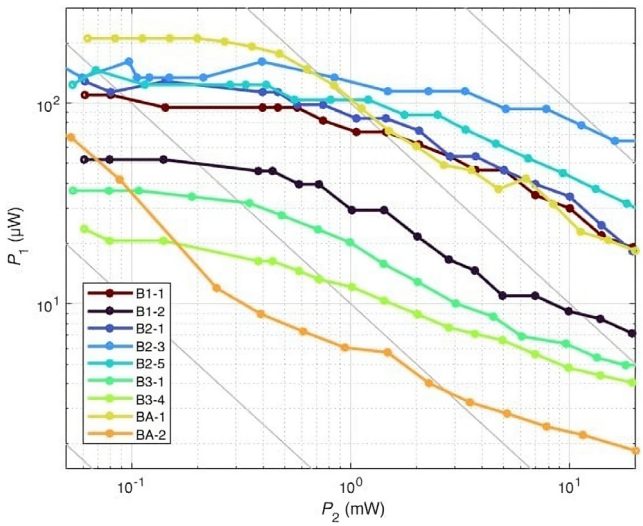

FIGURE 5 | Visualization of selected results from dosetests of the compounds **B1-1, B1-2, B2-1**, **B2-3**, **B2-5**, **B3-1,** and **B3-4** compared to biacetyl **BA-1** [13] and **BA-2** [12]. The power of the blue laser (vertical axis) is plotted against the power of the red laser (horizontal axis).

appearance in SEM images. Based on these observations, relative differences in line thickness can be identified, with broader lines indicating a stronger proximity effect linked to the corresponding photoinitiator [27]. All structures except **B2-3** were printed at a velocity of 1 mm/s. In contrast, **B2-3** required high laser power of 4.14 mW to achieve polymerization. Additionally, printing of fine structures was only possible at a reduced velocity of 0.5 mm/s. The need for both high laser power and low writing speed makes this initiator impractical for efficient 3D printing. For **B2-4**, the required laser power could not be determined because none of the printed structures adhered to the glass substrate and were displaced during the process (see Figure 3 in the Supporting Information). Repeated attempts under varying conditions yielded the same outcome, indicating that this initiator is an unreliable candidate for 3D laser nanoprinting. One possible explanation is that the strongly electron-withdrawing CF_3 substituents in B2-4 alter the aromatic core's electronic environment, reducing the initiation process's efficiency under available laser energy. This could lead to insufficient polymer formation at the substrate interface.

A closer examination of the surface reveals that the lines of the **B1-4** structure are noticeably thicker than those of the other structures. This means that the structure is overexposed. Typically, this can be adjusted by reducing the laser power. However, in this case, reducing the laser power from 0.64 to 0.32 mW did not result in photopolymerization of the photoresist.

Small particles are observed on and around the surface of the 3D structure of **B4-3**, the only soluble and printable *para*-bis-benzile-derivative. This can be attributed to the limited solubility of the photoinitiator. It is only fully soluble while stirred and heated and can recrystallize upon cooling if left on the substrate for extended periods.

The 3D structure printed with the lowest laser power was obtained using **B1-6**. The reduced laser power can be traced back to the strong positive mesomeric effect of the methoxy group. Due to this effect, the electron density in the aromatic system, and correspondingly the HOMO level, is increased, resulting in a lower energy threshold for radical formation. This finding, that substituents with a positive mesomeric effect reduce the required laser power, provides valuable guidance for the future design of benzil-based photoinitiators. Lower laser power is advantageous because it enables more energy-efficient printing, reduces stress on the optical setup, and facilitates the fabrication of delicate nanostructures. It also opens perspectives toward parallelization, e.g., by using multiple laser foci instead of only one, in which case the overall required laser power increases proportional to the number of foci [28].

Overall, the application of 3D laser nanoprinting via two-step absorption using only the blue 405 nm laser yielded fourteen soluble photoinitiators that produced optically well-resolved 3D structures. The required printing energy ranged from 0.16 to 4.23 mW, with particularly low thresholds under 1 mW observed for B1-6 (0.16 mW), B1-8 (0.48 mW), B1-4 (0.64 mW), and B4-3 (0.76 mW).

4 | Conclusion

In summary, twenty-three novel photoinitiators were synthesized. Fifteen of these could be used for the preparation of photoresists. Ultimately, fourteen could be used to print 3D structures with dimensions of 20 μm × 20 μm × 20 μm. This study provides new insights into the relationship between the structure of photoinitiators and their photopolymerization behavior, particularly regarding the energy required to initiate the photopolymerization.

The results highlight that, despite being less investigated than common two-photon absorption processes, two-step absorption can be a viable approach for creating micro- or even nanostructures, providing valuable structure-reactivity correlations that are currently lacking in this research area. Looking ahead, further molecular optimization and mechanistic studies could expand the scope of two-step photoinitiators and clarify how to utilize their unique excitation pathway for efficient, accessible 3D microfabrication. To this end, advances of quantum chemistry in regard to modeling these molecules and the processes happening during laser printing would be very highly desirable but are elusive at present.

Author Contributions

Aleksandra Vranic: conceptualization (lead), data curation (lead), formal analysis (lead), writing – original draft (lead), writing – review and editing (supporting). **Sarah Wulff:** investigation (supporting). **Pascal Rietz:** investigation (supporting). **Jonathan L. G. Schneider:** investigation (supporting). **Sophia Abou El Mirate:** investigation (supporting). **Martin Wegener:** funding acquisition (equal), supervision (equal), writing – review and editing (equal). **Stefan Bräse:** conceptualization (lead), funding acquisition (lead), supervision (lead), writing – review and editing (lead).

Acknowledgments

The authors acknowledge support from the Karlsruhe School of Optics & Photonics (KSOP). Financed by the Ministry of Science, Research and the Arts of Baden-Württemberg as part of the sustainability financing of the projects of the Excellence Initiative II. The authors acknowledge additional funding by the Deutsche Forschungsgemeinschaft (DFG, German Research Foundation) under Germany's Excellence Strategy for the Excellence Cluster "3D Matter Made to Order" (2082/1–390761711; 2082/2–390761711, Thrust A3 and B1), by the Carl Zeiss Foundation and by the Helmholtz program "Materials Systems Engineering."

Open Access funding enabled and organized by Projekt DEAL.

Funding

This work was supported by Deutsche Forschungsgemeinschaft (2082/1–390761711), Carl-Zeiss-Stiftung, Helmholtz Association, and Ministerium für Wissenschaft, Forschung und Kunst Baden-Württemberg.

Conflicts of Interest

The authors declare no conflicts of interest.

Data Availability Statement

The data that support the findings of this study are openly available in Chemotion at https://doi.org/10.1002/cptc.202500337, reference number 1.

References

1. S. Maruo and J. T. Fourkas, "Recent Progress in Multiphoton Microfabrication," *Laser & Photonics Reviews* 2 (2008): 100–111.

2. T. Baldacchini, *Three-Dimensional Microfabrication Using Two-Photon Polymerization* (Elsevier, 2016).

3. S. C. Gauci, A. Vranic, E. Blasco, S. Bräse, M. Wegener, and C. Barner-Kowollik, "Photochemically Activated 3D Printing Inks: Current Status, Challenges, and Opportunities," *Advanced Materials* 36 (2023): 2306468.

4. P. Somers, A. Münchinger, S. Maruo, C. Moser, X. Xu, and M. Wegener, "The Physics of 3D Printing with Light," *Nature Reviews Physics* 6, no. 2 (2023): 99–113.

5. C. W. Hull, "*Apparatus for Production of Three-Dimensional Objects by Stereolithography*," United States Patent, Appl., No. 638905, Filed, 1984.

6. M. Göppert-Mayer, "Elementary Processes with Two Quantum Transitions*," *Annalen der Physik (Berlin)* 18 (2009): 466–479.

7. S. Maruo and S. Kawata, "Two-Photon-Absorbed Near-Infrared Photopolymerization for Three-Dimensional Microfabrication," *Journal of Microelectromechanical Systems* 7 (1998): 411–415.

8. S. Maruo, S. Kawata, and O. Nakamura, "Three-Dimensional Microfabrication with Two-Photon-Absorbed Photopolymerization," *Optics Letters* 22, no. 2 (1997): 132–134.

9. V. Ferraro, C. R. Adam, A. Vranic, and S. Bräse, "Recent Advances of Transition Metal Complexes for Photopolymerization and 3D Printing under Visible Light," *Advanced Functional Materials* 34 (2023): 2302157.

10. C. N. LaFratta, J. T. Fourkas, T. Baldacchini, and R. A. Farrer, "Multiphoton Fabrication," *Angewandte Chemie International Edition* 46 (2007): 6238–6258.

11. V. Hahn, T. Messer, N. M. Bojanowski, et al., "Two-Step Absorption Instead of Two-Photon Absorption in 3D Nanoprinting," *Nature Photonics* 15 (2021): 932–938.

12. V. Hahn, P. Rietz, F. Hermann, et al., "Light-Sheet 3D Microprinting via Two-Colour Two-Step Absorption," *Nature Photonics* 16 (2022): 784–791.

13. N. M. Bojanowski, A. Vranic, V. Hahn, et al., "Search for Alternative Two-Step-Absorption Photoinitiators for 3D Laser Nanoprinting," *Advanced Functional Materials* 33, no. 39 (2022): 2212482.

14. P. V. Braun and M. L. Brongersma, "Photochemistry Democratizes 3D Nanoprinting," *Nature Photonics* 15 (2021): 871–873.

15. K. Sonogashira, Y. Tohda, and N. Hagihara, "A Convenient Synthesis of Acetylenes: Catalytic Substitutions of Acetylenic Hydrogen with Bromoalkenes, Iodoarenes and Bromopyridines," *Tetrahedron Letters* 16 (1975): 4467–4470.

16. K. Sonogashira, "Development of Pd–Cu Catalyzed Cross-Coupling of Terminal Acetylenes with sp^2-Carbon Halides," *Journal of Organometallic Chemistry* 653 (2002): 46–49.

17. J. K. Stille, "The Palladium-Catalyzed Cross-Coupling Reactions of Organotin Reagents with Organic Electrophiles [New Synthetic Methods (58)]," *Angewandte Chemie International Edition in English* 25 (1986): 508–524.

18. A. Gao, F. Yang, J. Li, and Y. Wu, "Pd/Cu-Catalyzed Oxidation of Alkynes into 1,2-Diketones Using DMSO as the Oxidant," *Tetrahedron* 68 (2012): 4950–4954.

19. B. N. Miyaura and A. Suzuki, "Stereoselective Synthesis of Arylated (E)-Alkenes by the Reaction of Alk-1-Enylboranes with Aryl Halides in the Presence of Palladium Catalyst," *Journal of the Chemical Society, Chemical Communications* (1979): 866–867.

20. N. Bruno, *Cross-Coupling Reaction Manual: Desk Reference* (2017).

21. J. P. Kuebrich, R. L. Schowen, M.-S. Wang, and M. E. Lupes, "The Mechanism of the Benzoin Condensation1,2," *Journal of the American Chemical Society* 93 (1971): 5.

22. M. B. Floyd, M. T. Du, P. F. Fabio, L. A. Jacob, and B. D. Johnson, "The Oxidation of Acetophenones to Arylglyoxals with Aqueous Hydrobromic Acid in Dimethyl Sulfoxide," *Journal of Organic Chemistry* 50 (1985): 5022–5027.

23. R. C. B. Alonso, W. C. Brandt, E. J. C. Souza-Junior, R. M. Puppin-Rontani, and M. A. C. Sinhoreti, "Photoinitiator Concentration and Modulated Photoactivation: Influence on Polymerization Characteristics of Experimental Composites," *Applied Adhesion Science* 2, no. 1 (2014): 10.

24. M. V. Encinas, E. Lissi, L. Gargallo, D. Radic, and R. Sigdman, "Polymerization Photoinitiated by Carbonyl Compounds. VI. Mechanism of Benzil Photoinitiation," *Journal of Polymer Science A1* 22 (1984): 2469–2477.

25. S. Dadashi-Silab, S. Doran, and Y. Yagci, "Photoinduced Electron Transfer Reactions for Macromolecular Syntheses," *Chemical Reviews* 116 (2016): 10212–10275.

26. M. Lang, S. Hirner, F. Wiesbrock, and P. Fuchs, "A Review on Modeling Cure Kinetics and Mechanisms of Photopolymerization," *Polymers* 14 (2022): 2074.

27. C. Arnoux, L. A. Pérez-Covarrubias, A. Khaldi, et al., "Understanding and Overcoming Proximity Effects in Multi-Spot Two-Photon Direct Laser Writing," *Additive Manufacturing* 49 (2022): 102491.

28. P. Rietz, P. Somers, S. Kalt, P. Kiefer, J. L. G. Schneider, and M. Wegener, "Parallelized Two-Step-Absorption 3D Laser Nanoprinting via Computational Holography Using a Digital Micromirror Device," *Laser 3D Manufacturing XII* (2025): PC133540C.

Supporting Information

Additional supporting information can be found online in the Supporting Information Section. **Supporting Fig S1:** Dosetest. Top: View of the generated preview. The dose test consists of 20 individual job files, in which the red laser power gradually increases from bottom to top. The blue laser power is kept constant within each job file, with a different blue power used for each file. Bottom: Optical dark-field image of the dose test after printing and development. The lowest point, or tip, of each printed structure corresponds to a data point of one curve in Figure 2. Each printing field is 100 μm width. **Supporting Fig. S2:** Graphical visualization of dosetest from every photoinitiator shown in this work. **Supporting Fig. S3:** Unedited 3D structures of all 1,2-diketones presented in Figure 5 of the main text, with the applied laser power indicated in mW. For B2-4, the left structure is shown without the corresponding laser power because the 3D structure flowed away and could not be assigned. Individual scale bars are provided at the bottom of each panel. For all images, the scale bars correspond to 5 μm.